UCRL-10438

University of California

Ernest O. Lawrence Radiation Laboratory

MECHANICS OF MOLECULAR PHOTODISSOCIATION

TWO-WEEK LOAN COPY

This is a Library Circulating Copy which may be borrowed for two weeks. For a personal retention copy, call Tech. Info. Division, Ext. 5545

DISCLAIMER

This document was prepared as an account of work sponsored by the United States Government. While this document is believed to contain correct information, neither the United States Government nor any agency thereof, nor the Regents of the University of California, nor any of their employees, makes any warranty, express or implied, or assumes any legal responsibility for the accuracy, completeness, or usefulness of any information, apparatus, product, or process disclosed, or represents that its use would not infringe privately owned rights. Reference herein to any specific commercial product, process, or service by its trade name, trademark, manufacturer, or otherwise, does not necessarily constitute or imply its endorsement, recommendation, or favoring by the United States Government or any agency thereof, or the Regents of the University of California. The views and opinions of authors expressed herein do not necessarily state or reflect those of the United States Government or any agency thereof or the Regents of the University of California.

UCRL-10438
UC-4 Chemistry
TID-4500 (19th Ed.)

UNIVERSITY OF CALIFORNIA

Lawrence Radiation Laboratory
Berkeley, California

Contract No. W-7405-eng-48

MECHANICS OF MOLECULAR PHOTODISSOCIATION

Richard N. Zare and Dudley R. Herschbach

February 1963

Printed in USA. Price $1.50. Available from the
Office of Technical Services
U. S. Department of Commerce
Washington 25, D.C.

MECHANICS OF MOLECULAR PHOTODISSOCIATION*

Richard N. Zare† and Dudley R. Herschbach

Department of Chemistry and Lawrence Radiation Laboratory,
University of California, Berkeley, California

Abstract

A computer program which provides the trajectories and velocity distributions of the atoms formed in photodissociation of a diatomic molecule is described. A table summarizing studies of fluorescence lines emitted by electronically excited product atoms is given, and the factors which determine the Doppler width of the fluorescence are discussed. It is shown that for ionic molecules a simple one-electron transfer model predicts that parallel and perpendicular electronic transitions should have comparable transition dipole moments, whereas for covalent molecules parallel transitions should dominate. A simple one-electron charge transfer model is applied to the np(M)$\rightarrow$n'p(X) transitions, which produce photodissociation of alkali halides accompanied by atomic alkali fluorescence. The model predicts that most of the intensity will appear in the perpendicular rather than the parallel components of these transitions.

*Support of this research by the Atomic Energy Commission and the Alfred P. Sloan Foundation is gratefully acknowledged.

†National Science Foundation Pre-doctoral Fellow.

INTRODUCTION

This report supplements a previous paper,[1] hereafter referred to as I, which developed a semiclassical treatment of the photodissociation of a diatomic molecule.

The probability of photodissociation is greatest when the electronic transition dipole moment $\underset{\sim}{\mu}_{if}$ of the molecule is aligned with the electric vector $\underset{\sim}{E}$ of the exciting light beam. Thus, since the excited electronic state usually dissociates in a time short compared with the molecular rotation, the angular distribution of the fragment atoms shows a corresponding anisotropy. It is peaked at right angles to the incident light beam if the transition moment is parallel to the internuclear axis (e.g., a Σ-Σ transition) or peaked forward and backward along the light beam if the moment is perpendicular to the axis (e.g., a Σ-Π transition).

The detailed form of the angular distribution is obtained by averaging the angular dependence of the transition probability, proportional to $|\underset{\sim}{\mu}_{if} \cdot \underset{\sim}{E}|^2$, over all rotational orientations of the molecule. Several distinct cases arise, specified by the <u>polarization</u> of the exciting light; by the orientation of $\underset{\sim}{\mu}_{if}$, which is either parallel or perpendicular to the molecular axis; and by the direction of departure of the product atom, which is regarded as undergoing either <u>axial recoil</u> along the initial direction of the molecular axis, or <u>transverse recoil</u> perpendicular to it. The general result can readily be synthesized from these two limiting cases for the recoil direction.

In I, the treatment was illustrated with calculations on the photodissociation of sodium iodide,

$$NaI + h\nu \rightarrow Na(^2P_{1/2} \text{ or } ^2P_{3/2}) + I(^2P_{3/2}),$$

in which an electronically excited sodium atom and an unexcited iodine atom are produced. This report presents these calculations more fully, including the Franck-Condon factors in the transition probability, statistical weights, and the trajectories and velocity distribution of the recoiling atoms.

If one of the product atoms is electronically excited, as in the case of NaI, it will radiate, and the contour of the atomic line may be strongly influenced by the mechanics of the photodissociation. The Doppler line shape for this atomic fluorescence has been derived in I, by projecting along the direction of observation the distribution of velocity vectors of the atom and averaging over the thermal motion of the center of mass of the parent molecule. The fluorescence width may greatly exceed ordinary thermal Doppler broadening, since the emitting atom often has a large recoil velocity. However, in cases for which the angular distribution is markedly anisotropic, much of the recoil broadening can be avoided by observing the fluorescence at right angles to the preferred direction of recoil. In the most favorable case (incident light polarized, $\underset{\sim}{\mu}_{if}$ parallel to the molecular axis, fluorescence viewed along the electric vector $\underset{\sim}{E}$), the predicted line shape is bimodal, and if one lobe were used a relatively narrow emission line could be obtained.

The Doppler line width is an important design parameter for proposed optical maser systems which would utilize the fluorescence of atoms produced by photodissociation.[2,3] Thus there is some interest in applying the criteria obtained in I to search for molecules which could yield a narrow atomic fluorescence line and which would be otherwise suitable for the maser application. Such a search is described in this report. Also, a bibliography is provided which lists all known experimental studies of atomic fluorescence excited by molecular photodissociation.

Unfortunately, for most molecules of interest, not enough is known about the excited electronic states involved in photodissociation to enable a definite prediction of the form of the angular distribution or the fluorescence line shape. The primary factor is just the relative importance of <u>parallel</u> (e.g., $\Sigma \rightarrow \Sigma$) and <u>perpendicular</u> (e.g., $\Sigma \rightarrow \Pi$) character in the excited states. However, usually there is more than one possible repulsive potential curve which leads to the same pair of separated atoms, and the curves for states of different symmetry may lie relatively close together. Since the exciting light often covers a broad band of frequencies, several different repulsive states may contribute to the photodissociation, and the relative transition probabilities for Σ–Σ and Σ–Π transitions appears to be an unresolved question at present.

These difficulties are illustrated here by a detailed discussion of the nature of the excited states for alkali halide molecules. A possible interpretation is given for some measurements of the intensity ratio of the D_1 and D_2 doublet lines in the alkali atom

fluorescence, which have shown that the ratio varies strongly with the energy of the light used to induce the photodissociation.[4]

CALCULATION OF RECOIL DISTRIBUTIONS

The distribution of the recoil velocity of the product atoms is the only factor in the calculation of the angular distribution or the Doppler line shape which depends on the detailed mechanics of photodissociation (See I, Section II). This recoil distribution is determined by the shape of the potential curves for the ground and excited electronic state of the parent molecule, the thermal distribution of initial rotational and vibrational energy, and the spectral distribution of the pumping light. The photodissociation of NaI will be treated in detail in discussing these factors and in describing the IBM 7090 computer program which has been prepared.

Excitation Probability

According to the Franck-Condon principle,[5] the probability that an electronic jump takes place from the ground level to a repulsive potential curve V(r) is proportional to

$$I_p \nu_p f_n \left| \int \psi_{n''}(r) \psi_{n'}(r) dr \right|^2, \tag{1}$$

where $\psi_{n'}$ is the vibrational wavefunction characterizing the unstable upper state, $\psi_{n''}$ is the wavefunction for the $\underline{n}^{th}$ vibrational level of the ground electronic state with energy E_n above the lowest level and relative population f_n; and the pumping light has intensity I_p at the frequency ν_p for which

$$V(r) = h\nu_p + E_n \tag{2}$$

Since the atoms in their vibrational motion stay a longer period of time in the neighborhood of the classical turning point than at some distance from it, a primitive approximation to the Franck-Condon principle is often used which assumes, for $n = 0$, that electronic jumps occur only vertically upward from the turning points of the classical vibration. For $n = 0$, the ground state vibrational wavefunction is a simple bell-shaped curve and the transition is assumed to occur only from the midpoint. This approximation was employed in the calculations given in I.

To improve on this, we must evaluate the square of the overlap integral,

$$\left| \int \psi_{n''}(r)\psi_{n'}(r)dr \right|^2. \tag{3}$$

Accurate repulsive eigenfunctions can be obtained from $V(r)$ by a numerical solution of Schrodinger's equation.[6] However, to avoid an elaborate calculation, we shall use a popular method first given by Winans and Stueckelberg.[7] The upper state repulsive eigenfunction is replaced by a delta function which is different from zero only at the classical turning points. Results obtained in this manner differ only very slightly from those obtained with correct repulsive wavefunctions as Coolidge, James and Present have shown in detail.[8] If $\psi_{n'}(r)$ is replaced in (2) by $\delta(r-r_o)$, the probability for an electronic transition occuring with internuclear distance between r_o and $r_o + dr_o$ becomes proportional to

$$I_p \nu_p f_n \left| \psi_n(r_o) \right|^2 dr_o. \tag{4}$$

For the first few vibrational levels of the ground state of NaI it is sufficient to use harmonic oscillator wavefunctions. The

transition probability (4) then becomes

$$I_p \nu_p f_n (2^n n!)^{-1} (\alpha/\pi)^{1/2} e^{-\xi^2} H_n^2(\xi) dr_o \tag{5}$$

Here $H_n(\xi)$ is the nth order Hermite polynomial,[9] $\xi = \sqrt{\alpha}(r_o - r_e)$ is proportional to the displacement from the equilibrium bond length r_e, and $1/\sqrt{\alpha}$ is the classical amplitude of vibration in the ground state, with

$$\alpha = 4\pi^2 \mu \omega_e c/h, \tag{6}$$

where μ is the reduced mass of the molecule and ω_e the vibration frequency. For NaI, $1/\sqrt{\alpha} = 0.078$, in Angstrom units.

Repulsive Potential Function

Figure 1 shows the repulsive potential curve for NaI, as derived by Hanson from fluorescence intensity measurements.[10] A portion of the potential curve for the ground state is also shown, including the vibrational levels and their relative populations. The threshold energy $V(\infty) = 5.22 \pm .09$ ev is the sum of the NaI dissociation energy ($D_o = 3.12$ ev) recommended by Brewer[11] and the Na(2p) excitation energy. The upper state potential curve was fitted to a best least squares 6th order polynomial in the range $r = 2.4615$ Å ($X = 0$) to $r = 2.9615$ Å ($X = 0.5$) where $V(X)$ is given in wave numbers:

$$\begin{aligned} V(X) = {} & 3.9549354\times10^6 X^6 - 6.7053816\times10^6 X^5 \\ & + 4.250458\times10^6 X^4 - 1.2435592\times10^6 X^3 \\ & + 1.944537\times10^5 X^2 - 3.7670057\times10^4 X \\ & + 4.9953698\times10^4 \end{aligned} \tag{7}$$

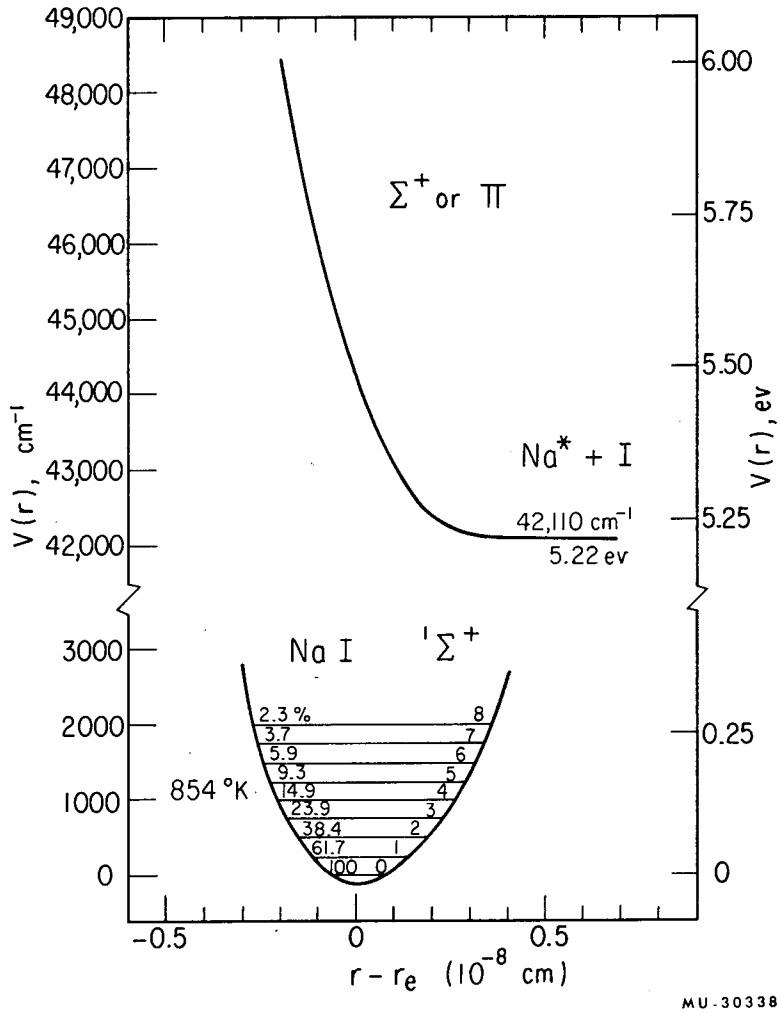

Fig. 1. Potential Curves for the NaI Molecule (After Hanson[10]).

Recoil Velocity

The relative kinetic energy of the separating Na and I atoms is given by

$$E = V(r_o) - V(\infty) + L^2/2\mu r_o^2 \tag{8}$$

where L is the rotational angular momentum of the NaI molecule. The recoil velocity of the atoms is

$$V_{Na}(r_o,n,L) = (m_I/m_{NaI})(2E/\mu)^{1/2} \tag{9a}$$

$$V_I(r_o,n,L) = (m_{Na}/m_{NaI})(2E/\mu)^{1/2} \tag{9b}$$

The computer program calculates the velocities for given values of r_o, n, and L. In the NaI calculations, for each vibrational level (n=0,1,2,3) the angular momentum was varied from 1 to 121 (in units of $\hbar = h/2\pi$) in intervals of 10 units, and for each pair of values of n and L, r ranged in steps of 0.1 Å from 2.46 Å to 2.96 Å.

The statistical weight $S(r_o,n,L)$ associated with a recoil velocity $V_{Na} = V_{Na}(r_o,n,L)$ is given by the product of the vibrational population factor f_n, the rotational population function f_L, and the normalized probability that a transition to the repulsive state will occur in a small interval about r_o. The relative values of f_n are given in Fig. 1 for a temperature of 854°K. To obtain the appropriate rotational statistical weight factor f_L, the relative population of the rotational levels f_J is divided by 2J+1, since the effect of orientational degeneracy has already been included in the "form factors" derived in I for the angular distribution. Thus,

$$f_L = (1.4387B/T)\mathrm{Exp}[-1.4387BJ(J+1)/T] \tag{10}$$

where for NaI the rotational constant B = 0.1177 cm^{-1}.

For a given vibrational state n and angular momentum L, the range of recoil velocities V_{Na} which corresponds to the transition probability (5) is given by

$$dV_{Na} = (V_{Na}/2E)(\partial E/\partial r_o)dr_o \tag{11}$$

where the second factor in the Jacobian is

$$\partial E/\partial r_o = (\partial V/\partial r)_o - L^2/\mu r_o^3. \tag{12}$$

Thus, on combining (5) with this Jacobian and the rotational weights we obtain the probability that the recoil velocity of the sodium atom is in the range from V_{Na} to $V_{Na} + dV_{Na}$ as

$$S(r_o n, L)dV_{Na} = \frac{2Ef_n f_L N_m^2 e^{-\alpha(r_o-r_e)^2} H_n^2[\sqrt{\alpha}(r_o-r_e)]}{V_{Na}(\partial E/\partial r_o)} dV_{Na} \tag{13}$$

Here N_m denotes the normalization factor included in (5). Graphs of the total statistical weight, $S(V_{Na},n)$, versus V_{Na} were prepared by having the computer accumulate the values of $S(r_o,n,L)$ corresponding to values of $V_{Na}(r_o,n,L)$ within small increments ΔV_{Na}, then smooth the resulting histograms. The $S(V_{Na},n)$ distribution is shown in Fig. 2, for the vibrational levels n = 0, 1, and 2.

Eq. (13) presumes a continuous light source with equal intensity per unit wavelength interval, but can be readily modified to apply to any pumping source whose spectral intensity distribution is known. The computer program also calculates from (2) the pumping wavelength required to produce each recoil velocity, $\lambda = hc/E$. The statistical weight associated with transitions produced by wavelengths within the range λ to $\lambda + d\lambda$ is obtained by replacing Eq. (11) with

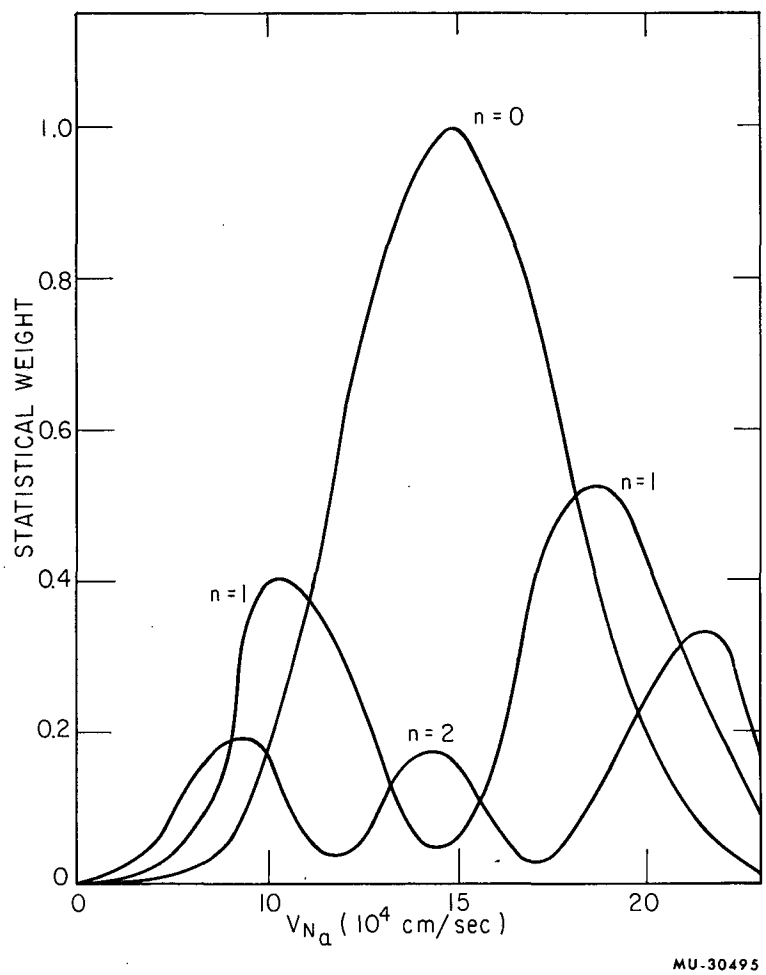

Fig. 2. Statistical weight for sodium recoil velocity.

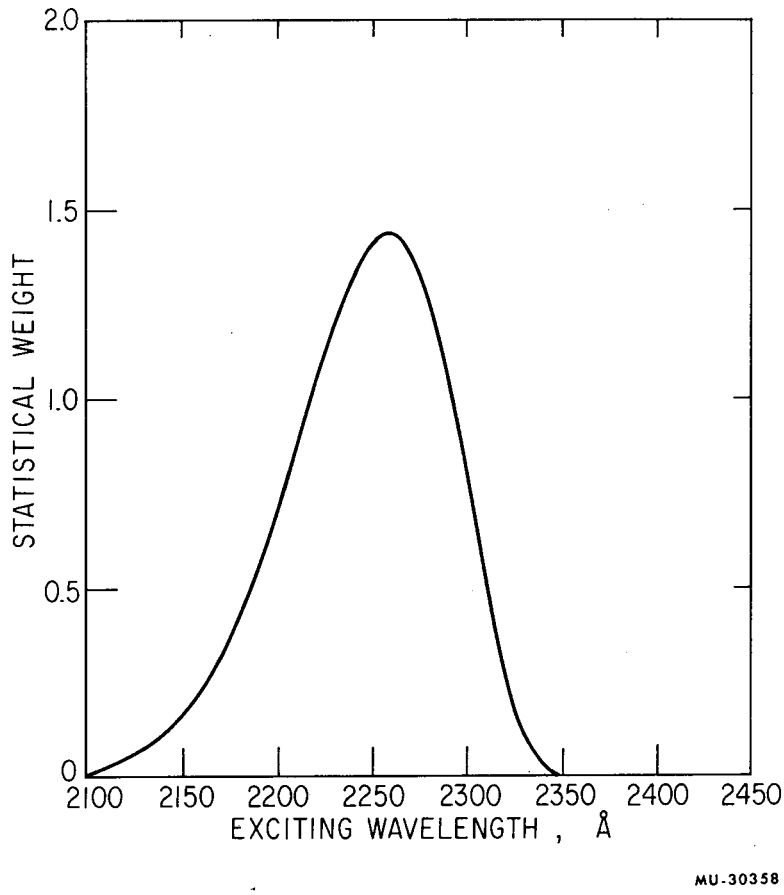

Fig. 3. Statistical weight for photodissociation dependence on wavelength of the light source.

$$d\lambda = (\lambda/E)(\lambda E/\lambda r_o)dr_o.$$

Thus Eq. (13) applies with dV_{Na} replaced by $d\lambda$ and the factor $(2/V_{Na})$ replaced by $(1/\lambda)$. The variation of the statistical weight for photodissociation with wavelength is shown in Fig. 3, for the n=0 vibrational level. For example, a pumping bandwidth of 40 Å will photodissociate over 35% of the n=0 level population with a velocity distribution between about 1.3×10^5 to 1.5×10^5 cm/sec.

Recoil Angle and Trajectory

Unless the recoil velocity is very large compared to the angular velocity of molecular rotation, the angular distribution of the products will be "smeared out" to some extent by the rotation. In I, this effect was evaluated in terms of the "recoil angle," χ. As indicated in Fig. 4, the line joining the separating Na^* and I atoms rotates from its initial direction (at t=0, when the photon is absorbed) and approaches asymptotically (at $t=\infty$) a line which makes an angle χ with the initial direction. In I it was shown that the angular distribution, $I(\theta)$, and the form factor, R_F, for the fluorescence line shape can be obtained by "mixing" the results for the simple limiting cases of purely axial and purely transverse recoil,

$$I(\theta) = I_A(\theta)\cos^2\chi + I_T(\theta)\sin^2\chi \tag{14}$$

$$R(v) = R_A(v)\cos^2\chi + R_T(v)\sin^2\chi \tag{15}$$

The recoil angle is obtained from

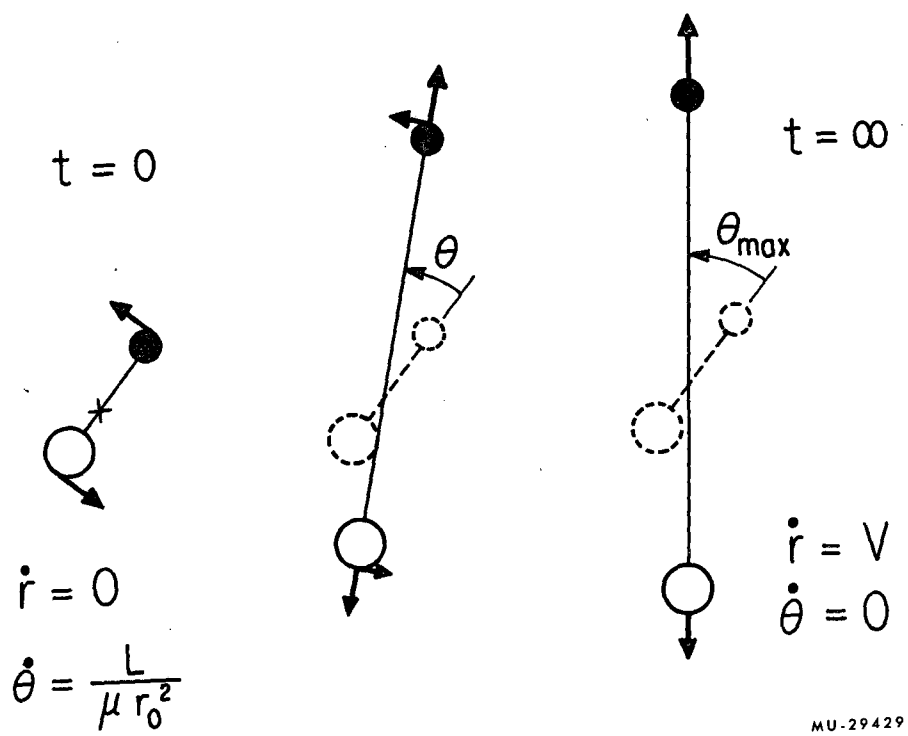

Fig. 4. Trajectory of recoiling products.

$$\chi(r_o,L) = (L^2/2\mu)^{1/2}\int_{r_o}^{\infty} \left[V(r_o)-V(r)+\frac{L^2}{2\mu}\left(\frac{1}{r_o^2}-\frac{1}{r^2}\right)\right]^{-1/2} \frac{dr}{r^2} \qquad (16)$$

As $r\to\infty$, the potential energy $V(r)$ approaches its limiting asymptotic value, $V(\infty)$. For convenience, we take $V(r_1) = V(\infty)$ at a suitable distance $r = r_1$; this considerably simplifies the numerical integration and introduces negligible error. For NaI, r_1 is about 3 Å. The total energy is

$$E = V(r_o) + L^2/2\mu r_o^2 = V(r_o) + W_o \ , \qquad (17)$$

the sum of the potential energy at the turning point and the "centrifugal energy," W_o, arising from the angular momentum. We choose the origin of the energy scale such that $V(\infty) = 0$. At any $r_2 > r_1$, the line of centers has rotated through the angle

$$\chi(r_2,r_o,L) = (L^2/2\mu)^{1/2}\int_{r_o}^{r_1} [E-V(r)-W(r)]^{-1/2} \frac{dr}{r^2}$$

$$+ \arccos\,(W_2/E)^{1/2} - \arccos\,(W_1/E)^{1/2}$$

As $r_2\to\infty$, $W_2\to 0$, and this slowly approaches the recoil angle,

$$\chi(r_o,L) = (L^2/2\mu)^{1/2}\int_{r_o}^{r_1} [E-V(r)-W(r)]^{-1/2} \frac{dr}{r^2}$$

$$+ \frac{\pi}{2} - \arccos(W_1/E)^{1/2} \qquad (18)$$

The computer program can also provide the actual trajectory and the "flight time." The rotation angle, $\chi(r,r_o,L)$, at each separation distance $r > r_o$ is obtained by integrating (16) from r_o to r rather than from r_o to ∞. The corresponding flight time is obtained from

$$t = \int_{r_o}^{r} \{(2/\mu)[E-V(r)-W(r)]\}^{-1/2} dr \tag{19}$$

where $t = 0$ at $r = r_o$; for $r_2 > r_1$ this becomes

$$t_2 = \int_{r_o}^{r_1} \{(2/\mu)[E-V(r)-W(r)]\}^{-1/2} dr$$

$$+ \frac{1}{v} [r_2(1-W_2/E)^{1/2} - r_1(1-W_1/E)^{1/2}] \tag{20}$$

where $v = (2E/\mu)^{1/2}$ is the final asymptotic velocity of separation of the atoms. A sample trajectory calculation is given in Table I.

Table I. Sample calculation of trajectory for n = 0, L = 51.

Angle (degrees)	Distance (cm)	Time (sec)
0.04	3.26×10^{-8}	2.3×10^{-14}
5.48	4.0	6.7
8.27	5.0	12.5
10.12	6.0	18.3
11.43	7.0	24.1
12.42	8.0	29.9
13.18	9.0	35.7
13.79	10.0	41.4
17.44	30.0	156.2
18.17	50.0	270.9
18.48	70.0	385.5
18.65	90.0	500.2
18.76	110.0	614.8
.	.	.
.	.	.
.	.	.
$19.25 \equiv \chi$	∞	∞

ATOMIC FLUORESCENE EXCITED BY MOLECULAR PHOTODISSOCIATION

A summary and bibliography of all known experimental studies of atomic fluorescence produced by molecular photodissociation is given in Table II. The wavelength of the atomic fluorescence lines is denoted by λ_F(Å), and the wavelength of the pumping light required to dissociate the molecule (in its ground vibrational state) and excite the fluorescence is denoted by λ_P(Å). The values of the dissociation energy D_o^o (ev) have been taken from Gaydon,[12] although in many cases more recent data are available. The indicated uncertainty in λ_P arises mainly from that in the D_o^o values.

Table II. Studies of Atomic Fluorescence Excited in Molecular Photodissociation.

Diatomic Molecule	λ_F(Å)	λ_P(Å)	D_o^o(ev)	References
LiBr	6708	2000±90	4.35±.3	13,14,15
LiI	"	2320±85	3.5 ±.2	13,14,15
Na_2	5896/90	4350±50	.75±.03	8,10
NaBr	"	2100±35	3.8 ±.1	3,5,12,13,14,15, 19,32
NaCl	"	1955±15	4.24±.05	5,12,32
NaI	"	2400±50	3.07±.1	1,2,3,4,5,6,7,9, 12,19,20,
	3303/02	1815±25		21,24,32,36,37
KBr	7699/65	2235±20	3.94±.05	3,5,12,32
KCl	"	2060±15	4.40±.05	3,5,12,32
KI	"	2515±25	3.32±.05	3,5,12,32
CuI	3274/48	2140±70	2.0 ±.2	7
RbBr	7948/7800	2215±90	4.0 ±.25	5,12
RbCl	" "	2035±65	4.5 ±.2	12,32
RbI	" "	2510±50	3.35±.1	5,12,20,22,30,31
AgI	3383	1980±80	2.6 ±.25	16,17,29
	3281	1945±75		
InBr	4511	2020±60	3.4 ±.2	33,34,35
	4105	1930±60		
InCl	4511	1740±25	4.5 ±.1	34,35
	4105	1670±20		
InI	4511	2240±75	2.8 ±.2	33,34,35
	4105	2130±70		
CsBr	8944/8521	2230±95	4.1 ±.25	5,12
	4593/55	1830±80		
CsCl	8944/8521	2045±65	4.6 ±.2	5,20
	4593/55	1705±45		
CsI	8944/8521	2555±50	3.4 ±.1	1,3,5,7,12,18,20
	4593/4551	2040±35		

(Continued)

Diatomic Molecule	λ_F(Å)	λ_P(Å)	D_o^o(ev)	References
TlBr	5351/3776	1945±30	3.2 ±.1	6,7,11,16,29
TlCl	5351/3776	1780±25	3.78±.1	7,11,16,29
TlI	5351/3776	2145±35	2.6 ±.1	6,7,11,16,23,26, 27,28,29
BiI	3068	1895±250	2.5 ±1	25

References for Table II

1926

1. V. Kondratjew, "Über Dissoziation heteropolarer Moleküle durch Lichtabsorption," Z. Physik 39, 191

2. A. Terenin, "Anregung von Atomen und Molekülen zur Lichtemission durch Einstrahlung. II," Z. Physik 37, 98

1927

3. J. Franck, H. Kuhn and G. Rollefson, "Beziehung zwischen Absorptionsspektren und chemischer Bindung bei Alkalihalogenid-dämpfen," Z. Physik 43, 155

4. T. R. Hogness and J. Franck, "Über den Nachweis der Relativ-geschwindigkeit der Zerfallsprodukte bei optischen Dissoziations-prozessen," Z. Physik 44, 26

5. L. A. Müller, "Absorptionsspektren der Alkalihalogenide in Wässeriger Lösung und im dampf," Ann. Physik 82, 39

6. A. Terenin, "Optische Dissoziation der Salzmolekule," Z. Physik 44, 713

1928

7. K. Butkow and A. Terenin, "Optische Anregung und Dissoziation einiger Halogensalze," Z. Physik 49, 865

8. F. W. Loomis and S. W. Nile, "New Features of the Red Band System of Sodium," Phys. Rev. 32, 873

9. A. C. G. Mitchell, "Über die Richtungsverteilung der Relativ-geschwindigkeit der Zerfallsprodukte bei der optischen Dissoziation von NaJ," Z. Physik 49, 228

10. R. W. Wood and E. L. Kinsay, "The Fluorescence Spectrum of Sodium Vapor in the Vicinity of the D-Lines," Phys. Rev. 31, 793

1929

11. K. Butkow, "Absorptionsspektren und Art der chemischen Bindung der Thallohalogenide im Dampfzustande," Z. Physik 58, 232

12. K. Sommermeyer, "Ein neues Spektrum der gasförmigen Alkalihalogenide und seine Deutung," Z. Physik 56, 548

13. A. Terenin, "Über die optische Dissoziationswarme von Salzdämpfen," Physica 9, 283

14. G. H. Visser, "Optische Bepaling van de Dissociatiewarmte van Zoutdampen," Physica 9, 115

15. G. H. Visser, "Optische Dissoziation von Salzdämpfen," Physica 9, 285

1930

16. A. Terenin, "Photoionization of Salt Vapors," Phys. Rev. 36, 147

17. A. Terenin, "Dissociation Fluorescence of AgI Vapour," Physica 10, 209

18. G. H. Visser, "Notiz zur optischen Dissoziation des CsJ," Z. Physik 63, 402

19. J. G. Winans, "Die Auslöschung der Natrium fluoreszenz durch Fremdgase," Z. Physik 60, 631

20. H. D. Schmidt-Ott, "Über kontinuierliche Absorptionsspektren des gasförmigen Alkalihalogenide im U V ," Z. Physik 69, 724

21. A. Terenin and N. Prileshajewa, "Der Wirkungsquerschnitt der Auslöschung der Na-Emission durch Jodatome und Moleküle," Zeit. Phys. Chem. B13, 72

22. G. H. Visser, "Über die Einwirkung des Lichtes auf Rubidiumjodiddampf," Z. Physik 70, 605

1932

23. J. M. Frank, "Die Anregungsfunktion und die Absorptionskurve bei der optischen Dissoziation von TlJ," Phys. Zeit. Sowjet 2, 319

24. B. Kisilbasch, V. Kondratjew, and A. Leipunsky, "Die Auslöschung der Atomfluoreszenz," Phys. Zeit. Sowjet 2, 201

25. H. Neujin, "Photodissoziation des BiJ_3-Dampfes," Phys. Zeit. Sowjet 2, 422

26. N. Prileshajewa, "Auslöschung der Thallium-Fluoreszenz Durch Jod-Moleküle und Atome," Phys. Zeit. Sowjet, 2, 351

27. N. Prileshajewa, "Auslöschung der Tl-Fluoreszenz Durch TlJ-Moleküle, Phys. Zeit. Sowjet 2, 367

28. A. Terenin, "Emission Bands Excited in TlI Vapor by Ultraviolet Light," Phys. Zeit. Sowjet 2, 377

29. A. Terenin and B. Popov, Photodissociation of Salt Molecules into Ions," Phys. Zeit. Sowjet 2, 299

1933

30. M. S. Desai, "Über die Einwirkung des Lichtes auf Rubidiumjodiddampf," Z. Physik 85, 360

31. G. H. Visser and A. C. S. van Heel, "Über die Einwirkung des Lichtes auf Rubidiumjodiddampf," Z. Physik 86, 694

1934

32. H. Beutler and H. Levi, "Berechnung der Dissoziationswärme von gasformigen (sic) KCl, KBr, KJ, NaCl, NaBr, NaJ und LiJ in die atome aus thermischen und optischen Daten," Zeit. Phys. Chem. B24, 263

33. J. Sedov and A. Filipov, "Optical Dissociation of InBr and InI," Akademiia Nauk, Doklady Novaia Seriia Tom IV Vol. IV, 376

34. M. Wehrli and E. Miescher, "Spektroskopische Untersuchung dampfförmiger Indiumhalogenide," Helv. Phys. Acta 7, 298

After 1934

35. W. Wenk, "Absorptions- und Fluoreszenzspektra dreiatomarer Indium- und Gallium- Halogenide," Helv. Phys. Acta 14, 355, 1941.

36. H. G. Hanson, "Quenching of NaI Fluorescence by H_2, HCl, CO_2, and H_2O," J. Chem. Phys. 23, 1391, 1955.

37. H. G. Hanson, "Fluorescence Intensity Ratio of Sodium Doublet Observed in the Optical Dissociation of Sodium Iodide Vapor," J. Chem. Phys. 27, 491, 1957

POSSIBLE MASER SYSTEMS

As there is some interest in proposed optical maser systems[2,3] which would utilize the fluorescence of atoms produced by photodissociation, we shall briefly survey the possibilities. First we look for elements for which the excess energy required to excite an atomic level is no more than about 5 ev. above the threshold energy for dissociation of the molecule into normal unexcited atoms. Excitation produced by higher energy photons is likely to cause photoionization rather than photodissociation. After examining the diatomic molecules[13] formed from each atom which has an allowed transition within 5 ev. above the ground state,[14] we conclude that the only suitable elements are the alkali metals, copper, silver, indium, and thallium. These are just the atoms whose fluorescence has already been observed (see Table II). Although most other metals do possess the requisite low-lying excited electronic states, their valency of two or higher does not permit them to form diatomic molecules suitable for the maser application. The oxides, carbides, and sulfides, for example, are quite refractory and involatile, whereas the monohalides of divalent metals are very reactive and can only be formed in low concentration and under extreme conditions. Triatomic compounds such as the dihalides, MX_2, are also not promising, as they appear to dissociate invariably to an excited diatomic molecule and a halogen atom,[15] $MX_2 + h\nu \rightarrow MX^* + X$. The fluorescence spectrum from excited molecules is quite broad, and thus seems unlikely to prove suitable for a maser.

Among the various diatomic molecules formed from the monovalent metals, we should choose those which will yield an atomic line with a minimum Doppler width.[1-3] Three factors contribute to the Doppler width and may be considered separately: (1) the thermal center-of-mass motion of the molecule; (2) the recoil velocity (relative to the molecular center-of-mass) of the emitting atom; and (3), the angular distribution of the recoil velocity vectors.

Contribution (1) is usually the least important; it is less than the Doppler broadening for an atomic gas at the same temperature by a factor equal to the square root of the ratio of the mass of the atom to that of the molecule.

Contribution (2) can be minimized by using pumping light with energy only slightly above the threshold for photodissociation. However, since the most populated vibrational levels of the ground electronic state usually lie under a strongly sloping portion of the upper, repulsive potential curve, electronic jumps from these levels only occur for pumping light well above the threshold. Therefore pumping near the threshold involves a very substantial sacrifice of intensity and is impractical.

Another means of limiting the recoil velocity is to use a molecule AB for which the mass of the fluorescent atom, A, is much larger than that of its partner, B. As seen in Eq. (9), the recoil velocity of A is given by

$$\left(\frac{2m_b}{m_A m_{AB}}\right)^{1/2} E^{1/2}, \tag{21}$$

where E is the relative kinetic energy of separation of A and B.

Unfortunately, in the gas phase the hydrides of the monovalent metals are largely dissociated, as the equilibrium

$$2\ MH \rightleftharpoons 2M + H_2$$

favors M and H_2 at the relatively low pressures suitable for masers. In addition to the low concentration of MH, the presence of the metal atoms is also a serious handicap to maser action, since the emission from excited M^* atoms would be strongly absorbed and re-emitted by the background M atoms (unless the fluorescence of M^* is not a transition to the ground electronic state). The fluorides and chlorides of the monovalent metals also do not appear promising. These compounds have very strong bonds and in most cases the photodissociation would require pumping in a region of the vacuum ultraviolet for which only feeble sources are available.

Although there is no obvious choice of a molecule which would minimize (2), in some cases it may be possible to offset this by exploiting the anisotropic angular distribution (3) of the recoil vectors. As illustrated in I (Fig. 7), under the proper conditions a relatively narrow line may be obtained (from one lobe of a bimodel contour) by viewing the fluorescence at right angles to the preferred direction of recoil. However, the anisotropy is only pronounced when the photodissociation is produced by a parallel transition (e.g., a $\Sigma \rightarrow \Sigma$ rather than a $\Sigma \rightarrow \Pi$ transition). Unfortunately, as illustrated below, in most cases of interest several potential curves contribute to photodissociation, and it is not possible to predict beforehand whether parallel or perpendicular character will predominate.

We conclude that, by default, the diatomic bromides and iodides of the monovalent metals probably should be regarded as the leading prospects for a photodissociation maser. The volatility of the TℓBr and TℓI molecules makes them particularly attractive, whereas RbI and CsI offer the advantage that the requisite pumping region is readily accessible to strong ultraviolet light sources.

EXCITED ELECTRONIC STATES OF DIATOMIC MOLECULES

The symmetry of the molecular electronic states which may contribute in a photodissociation can be determined from well-known procedures,[13] and these will be outlined here. We may start with given states of the two separated atoms and ask which molecular states arise from them. When two atoms approach each other, an electric field arises in the direction of the line joining the nuclei. At first the electric field is relatively weak and the coupling between the orbital and spin angular momentum vectors, $\underset{\sim}{L}_i$ and $\underset{\sim}{S}_i$, in the separated atoms is stronger than the coupling of the $\underset{\sim}{L}_i$ to the internuclear axis. Consequently a space quantization of the total angular momentum vectors, $\underset{\sim}{J}_i = \underset{\sim}{L}_i + \underset{\sim}{S}_i$, occurs. This leads to (J_1,J_2) coupling. As the atoms approach closer, the strength of the electric field increases and a decoupling of the $\underset{\sim}{L}_i$ and $\underset{\sim}{S}_i$ vectors takes place. This produces a space quantization of $\underset{\sim}{L}_1$ and $\underset{\sim}{L}_2$ with respect to the internuclear axis, leading to (Λ,S) coupling.

For cases where Russell-Saunders coupling is valid for the separate atoms as well as the molecule, Wigner and Witmer[16] have derived a set of rules showing how (Λ,S) coupling arises from

$L_1S_1L_2S_2$ values of separated atoms. Most of the results given by these rules can be obtained in a straightforward manner by assuming negligible (L,S) coupling in the atoms and determining the possible values of the projections, M_{L_1} and M_{L_2}, of the $\underset{\sim}{L}_1$ and $\underset{\sim}{L}_2$ vectors on the internuclear axis. The resultant gives the possible Λ values, $\Lambda = M_{L_1} + M_{L_2}$. The S values, which determine the multiplicity, are simply $S_1 + S_2$, $S_1 + S_2 - 1$, ... , $|S_1 - S_2|$, and apply to each M_{L_1}, M_{L_2} combination. When $\Lambda = 0$, it is necessary to distinguish between Σ^+ and Σ^- states and this depends on the parity (odd or even) of the separated atoms. These results are applicable to all Hund coupling Case a or b molecules.

For cases where (J_1, J_2) coupling obtains in the atoms, Mulliken[17] has investigated how the J values of the separated atoms correlate with the symmetry of the molecular states of Hund's coupling Case c. Again, by similar considerations, the Ω values result from the possible projection of J_1 and J_2 on the internuclear axis, $\Omega = |M_{J_1} + M_{J_2}|$. When $\Omega = 0$, the determination of the 0^+ and 0^- states depend on parity considerations analogous to those for $\Lambda = 0$ in Russell-Saunders coupling. In both (Λ, S) and (J_1, J_2) coupling, if the molecule is formed from like atoms, the inversion symmetry (g or u) of the resulting molecular states must be determined.

We are particularly interested in the upper electronic states of the bromide and iodide diatomic molecules formed from the alkali metals, copper, silver, indium and thallium. We might expect these ionic molecules to show intermediate behavior between Hund's coupling Case c and Hund's coupling Case a or b. For sufficiently small values of r, the molecules will show Case a or b coupling,

while at large values of r, Case c coupling obtains. As a consequence, in photodissociation of these molecules the frequency of the pumping light will affect the symmetry of the upper state and hence the angular distribution and fluorescence line shape. For a pumping frequency close to the threshold, transitions are induced with large internuclear separation whereas pumping light of higher frequency favors transitions at smaller internuclear separation.

We wish to establish a correlation between (J_1, J_2) and (Λ, S) coupling with decreasing internuclear separation. This correlation can be accomplished by use of a "non-crossing rule." The lowest 0^+ state for large r is identified with the lowest 0^+ state for small r, the next lowest 0^+ for large r with the next lowest 0^+ state for small r, etc. Each other type of state (0^-, 1, 2, etc.) is treated in the same way.

To apply the non-crossing rule we must determine which symmetry states Σ^+, Σ^-, Π, Δ, etc. in Case a or b coupling correspond to which symmetry states 0^+, 0^-, 1, 2, etc. in Case c coupling. The identification can be best accomplished in terms of the total electronic angular momentum quantum number, Ω, which is defined for both Case c and a or b coupling. For Case a or b coupling it is given simply by

$$\Omega = |\Lambda + S|$$

All states with $\Omega = 0$ (for $\Lambda \neq 0$) split into 0^+ and 0^- components (Λ doubling). All other states with the exception of Σ states go according to their possible Ω values. The symmetry property g or u is also maintained. Mulliken[17] has tabulated the less obvious correlations of the Σ states and they are given in Table III.

Table III. Correlation of the Σ states between (Λ,S) and (J_1,J_2) coupling.

(Λ,S)	(J_1,J_2)
$^1\Sigma^+$; $^1\Sigma^-$	0^+; 0^+
$^2\Sigma^+$; $^2\Sigma^-$	$\frac{1}{2}$; $\frac{1}{2}$
$^3\Sigma^+$; $^3\Sigma^-$	$0^-,1$; $0^+,1$
$^4\Sigma^+$; $^4\Sigma^-$	$\frac{1}{2},\frac{3}{2}$; $\frac{1}{2},\frac{3}{2}$
$^5\Sigma^+$; $^5\Sigma^-$	$0^+,1,2$; $0^-,1,2$

We illustrate the foregoing by considering the molecular states of NaI in detail. In particular, we are not interested in the first low-lying electronic states, but rather only those electronic states which dissociate into an excited sodium atom $Na(^2P_{1/2},{}^2P_{3/2})$, which emits the sodium D doublet. On dissociation the iodine atom can be either in its normal state $^2P_{3/2}$ or in the metastable state $^2P_{1/2}$ having 22 Kcal per mole additional energy. We note that while the different electronic states of iodine are spaced far apart, the sodium doublet levels are only about 6 Å apart.

In the order of increasing energy we find for (J_1,J_2) coupling:

$$Na(^2P_{1/2}) + I(^2P_{3/2}) \longrightarrow 2,\ 1(2),\ 0^+,\ 0^-$$

$$Na(^2P_{3/2}) + I(^2P_{3/2}) \longrightarrow 3,\ 2(2),\ 1(3),\ 0^+(2),\ 0^-(2)$$

$$Na(^2P_{1/2}) + I(^2P_{1/2}) \longrightarrow 1,\ 0^+,\ 0^-$$

$$Na(^2P_{3/2}) + I(^2P_{1/2}) \longrightarrow 2,\ 1(2),\ 0^+,\ 0^-$$

where the number of each repeated state is given in parentheses after the state designation. For (Λ,S) coupling:

$$Na(^2P_u) + I(^2P_u) \longrightarrow {}^1\Sigma^+(2), {}^3\Sigma^+(2), {}^1\Sigma^-, {}^3\Sigma^-, {}^1\Pi(2), {}^3\Pi(2), {}^1\Delta, {}^3\Delta$$

For the sake of illustration, let us arbitrarily assume that the order of these molecular states for Case a or b coupling is ${}^1\Sigma^+$, ${}^1\Pi, {}^3\Sigma^+, {}^1\Delta, {}^1\Sigma^-, {}^1\Sigma^+, {}^1\Pi, {}^3\Sigma^+, {}^3\Pi, {}^3\Delta, {}^3\Sigma^-, {}^3\Pi$. The reasons for the particular choice will be considered later. Figure 5 shows the resulting correlation diagram.

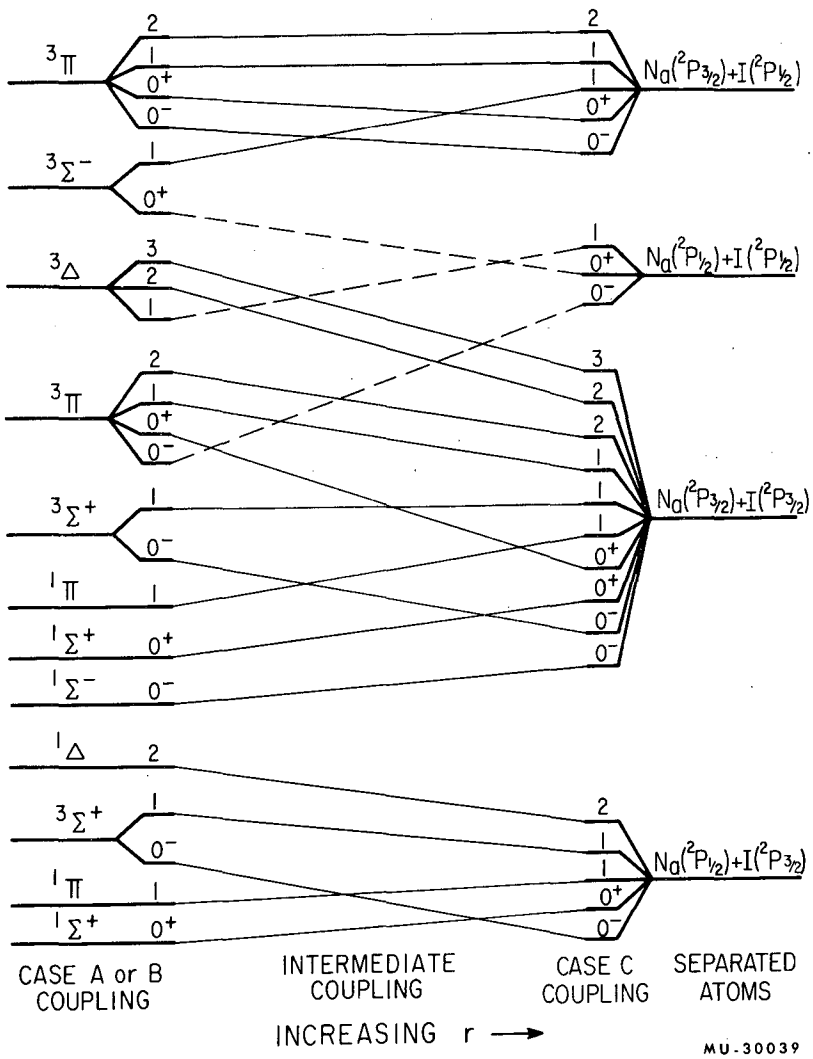

Fig. 5. Correlation diagram for the upper electronic states of NaI. The spacing of the energy levels has been grossly distorted for purposes of illustration.

Of course, the correlation depends critically on the ordering of the molecular states. In general, this can not be predicted a priori although often there will be some level for which a unique correlation exists, such as

$$^3\Delta \longleftrightarrow {}^3\Delta_3 \longleftrightarrow 3 \longleftrightarrow Na(^2P_{3/2}) + I(^2P_{3/2}).$$

For NaI the ordering of the upper electronic levels is completely unknown. There are 12! ways of arranging these levels, disregarding the ordering of the multiplicity, which also is unknown. (Of course, not all these choices of ordering will lead to different correlations.)

Since in the case of NaI the separation between the $Na(^2P_{1/2})$ and $Na(^2P_{3/2})$ atomic energy levels is quite small, all the repulsive potential curves going to a particular iodine atom (normal or metastable) will be closely bunched together and it will be impossible to excite only one upper state energy level without exciting the others lying nearby. Therefore, there appears to be no way to avoid exciting both members of the D doublets. Similarly, there appears to be no way of exciting only a $\Sigma - \Sigma$ transition, if there are also Π states lying nearby.

INTENSITY RATIO OF DOUBLET LINES IN ALKALI ATOM FLUORESCENCE

Recently H. G. Hanson[4] has conducted some experiments on the NaI photodissociation that have a bearing on the nature of the upper electronic levels. He measured the intensity ratio $D_2(^2P_{3/2})/D_1(^2P_{1/2})$ of the atomic sodium doublet components emitted in fluorescence, for different wavelengths of the ultraviolet light

inducing photodissociation. He found that at short wavelengths the D_2/D_1 ration was 0.98 and increased to 1.5 at longer exciting wavelengths. A similar effect was reported by Terenin[18] for the Ag doublet emitted in the photodissociation of AgI. The intensity ratio for the Ag doublet shows a large reversal, being considerably less than unity at short wavelengths and greater than unity at long wavelengths. However, the data for AgI is less quantitative because the energy separation of the doublets is much larger than that for NaI and only plate blackenings are reported. The phenomenon is probably general, and not peculiar to just NaI or AgI.

Hanson also studied the Doppler broadening of the two D lines by comparing the absorption of each line in passing through a layer of sodium vapor. Within experimental error, the ratio of absorption of the D_2 to the D_1 line was 2:1 at all incident wavelengths; thus no appreciable difference in the individual Doppler broadening of the two D lines was detected.

The intensity ratio of D_2 to D_1 is given by

$$\frac{D_2}{D_1} = \frac{\sum_x \left| \int \psi_{g_{e\ell}} \underset{\sim}{\mu} \psi_{x_{e\ell}} d\tau_e \int \psi_{g_v} \psi_{x_v} dr \right|^2}{\sum_y \left| \int \psi_{g_{e\ell}} \underset{\sim}{\mu} \psi_{y_{e\ell}} d\tau_e \int \psi_{g_v} \psi_{y_v} dr \right|^2}$$

Here $\psi_{g_{e\ell}}$ and ψ_{g_v} are respectively the electronic and vibrational wavefunctions of the ground state. The x states lead to the D_2 component of the doublet and the y states to D_1. The electronic dipole transition moment connecting the upper and ground state is denoted by $\underset{\sim}{\mu}$. If, as in treating the Franck-Condon overlap factors, we replace the vibrational wavefunctions of the repulsive state by

delta functions, the intensity ratio reduces to

$$\frac{D_2}{D_1} = \frac{\sum_x \left| \int \psi_{g_{e\ell}} \underset{\sim}{\mu} \psi_{x_{e\ell}} d\tau_e \right|^2}{\sum_y \left| \int \psi_{g_{e\ell}} \underset{\sim}{\mu} \psi_{y_{e\ell}} d\tau_e \right|^2} ,$$

which depends solely on the nature of the electronic wavefunctions.

From the correlation diagram of Fig. 5 it is seen that for dissociation into an excited sodium atom and a normal iodine atom five potential curves are D_1 active while ten are D_2 active. However, since there can be no allowed dipole transition connecting the ground state ($^1\Sigma^+$) to any Δ level, or any $^3\Pi$ component, 11 potential curves at most are active in emission, 7 or less D_2 active and 4 or less D_1 active.

For Case c coupling the selection rules for a dipole transition are simply

$$\begin{array}{l} \Sigma \longleftrightarrow \Sigma \\ \Sigma \longleftrightarrow \Pi \\ + \longleftrightarrow + \\ - \longleftrightarrow - \end{array} \qquad \text{and } \Delta J = 0, \pm 1$$

If we assume that all $\Sigma - \Sigma$ and $\Sigma - \Pi$ transitions are roughly of comparable strength for large r in Case c coupling, the D_2/D_1 ratio will generally be greater than 1 due to the predominance of potential curves D_2 active. However, at shorter wavelengths the stricter selection rules of Case a or b coupling would apply

$$^1\Sigma^+ \longleftrightarrow {}^1\Sigma^+$$

$$^1\Sigma^+ \longleftrightarrow {}^1\Pi$$

Transitions not allowed by Case a or b coupling will decrease in intensity as the internuclear separation is diminished. Thus, a possible interpretation can be offered for Hanson's experimental findings provided certain assumptions are made about the relative strength of the $\Sigma - \Sigma$ and $\Sigma - \Pi$ transitions. To account for the experimental observation that the ratio of D_2/D_1 is nearly unity (0.98) at small values of r_o, we assume that there is one set of $^1\Sigma^+$ and $^1\Pi$ levels D_1 active and one set D_2 active. If the transitions $^1\Sigma^+ \longrightarrow {}^1\Sigma^+$ and $^1\Sigma^+ \longrightarrow {}^1\Pi$ were of about equal intensity, other assignments would be possible, but they would contradict the observation that the Doppler broadening of the two doublet components is the same. At large internuclear separation, where Case c coupling obtains, it seems reasonable to assume that all $\Sigma \longrightarrow \Sigma$ and $\Sigma \longrightarrow \Pi$ transitions have roughly the same intensity. The D_2/D_1 ratio of 1.5 could then be explained by a 3 to 2 ratio in the number of potential states D_2 and D_1 active. We also make the relative number of Σ and Π components active for D_2 the same as that for D_1, so that there can be no difference in the Doppler broadening of the two doublet components. The correlation diagram presented in Fig. 5 has been constructed to correspond to these relationships.

The correlation diagram is still not uniquely determined by these assumptions, although there is little freedom of choice for the lower levels. Additional experiments suggest themselves. From a study of the D_2/D_1 ratio and the comparative Doppler broadening of these two components for dissociation into an excited sodium atom and a metastable iodine atom at different pumping light frequencies, it should be possible to obtain more information about the nature of

the upper potential states, which would perhaps lead to a unique correlation. Another experiment of interest would be to investigate more thoroughly the Ag doublet components, especially their relative Doppler broadening. To account for the dramatic reversal in intensity ratio at small r that Terenin observed, it appears that we must either postulate that the $^1\Sigma^+$ and $^1\Pi$ states are unequally divided among the doublet components, or that the $^1\Sigma^+ \longrightarrow {}^1\Sigma^+$ and $^1\Sigma^+ \longrightarrow {}^1\Pi$ transitions are not of equal intensity. In either case, we would expect that the Doppler broadening of the two doublet components would be different.

TRANSITION DIPOLE MOMENTS

As emphasized above, the primary factor which determines the form of the angular distribution of products in photodissociation and the shape of the atomic fluorescence line is just the relative importance of <u>parallel</u> (e.g., $\Sigma \rightarrow \Sigma$) and <u>perpendicular</u> (e.g., $\Sigma \rightarrow \Pi$) character in the electronic transition or transitions which produce the photodissociation. Unfortunately, it does not seem possible to make a reliable prediction of this, especially for molecules such as alkali halides, in which several different repulsive states may contribute to the photodissociation. Here we shall review the scanty evidence concerned with this question and present results derived from a simple charge transfer model.

A treatment of the hydrogen molecule-ion, H_2^+, by Bates and coworkers[19] is the only calculation we have found in the literature which permits the transition dipole moment to be compared for parallel and perpendicular transitions. They found that at the equilibrium

internuclear distance the transition dipoles for the $\Sigma_g^+ \rightarrow \Pi_u$ ($1s\sigma_g \rightarrow 2p\pi_u$) and the $\Sigma_u^+ \rightarrow \Pi_g$ ($2p\sigma_u \rightarrow 3d\pi_g$) <u>perpendicular</u> transitions were about equal in magnitude and about half as large as the dipole for the $\Pi_u \rightarrow \Pi_g$ ($2p\pi_u \rightarrow 3d\pi_g$) <u>parallel</u> transition.

Mulliken[20] has made an extensive study of the low-lying electronic states of simple diatomic halides, X_2, HX, MX, and in particular he has examined the dissociation of NaI into a normal sodium atom and a normal or metastable iodine atom. As may be seen from Fig. 5, this is a much simpler case, with fewer electronic states, than we have considered. However, the situation is still inconclusive:

> "...we conclude that strong transitions definitely should occur to the two 0^+ levels, the one derived from $X(^2P_{3/2})$, the other from $X(^2P_{1/2})$. This is in rough agreement with what is observed, if we ascribe the two continua essentially to $0^+ \leftarrow N$ transitions. In addition, there should be transitions to the three $\Omega = 1$ levels. If these should be weak, their superposition on two strong $0^+ \leftarrow N$ continua would scarcely be noticed. Even if they are fairly strong, they need not much affect the appearance of the continuous spectrum, provided the several levels derived from $M+X(^2P_{3/2})$ lie close together, and those from $M+X(^2P_{1/2})$ again close together. The evidence from Levi's analysis of the pseudo-bands indicates that transitions of appreciable intensity occur to at least two potential curves derived from $M+X(^2P_{3/2})$. Assuming that one of these is to the 0^+ state, the others (theoretically there must be <u>two</u> others, though only one was definitely detected by Levi's analysis) must be to $\Omega = 1$ states. Thus it seems likely that transitions to 0^+ and 1 states may be of comparable intensity. Theoretically, from a consideration of the probable forms of the wave functions, it appears likely that transitions to the 0^+ states should be the stronger."

Thus, according to Mulliken's analysis of the spectra (in contrast to his theoretical expectation), it appears that the $\Sigma \rightarrow \Sigma$ and $\Sigma \rightarrow \Pi$ transitions which produce a normal sodium atom are of comparable intensity in NaI. Likewise, Mitchell's evidence for an isotropic angular distribution of photodissociation products[21] and Hanson's observation of identical Doppler broadening for the sodium D doublets[4] suggest that the $\Sigma \rightarrow \Sigma$ and $\Sigma \rightarrow \Pi$ transitions which produce an excited sodium atom are also comparable in intensity. This is all rather circumstantial evidence, however.

We have considered a simple charge transfer model for transitions which produce photodissociation of an alkali halide molecule with excitation of the alkali atom. The model, of course, may be an inadequate approximation, but it is so simple that the results derived from it have some interest in their own right, especially since they seem to contradict "intuition." Thus, for an ionic molecule a charge transfer model might be expected to favor strong parallel transitions in which the electron would oscillate along the internuclear axis in resonance with the exciting light. However, numerical calculations for the LiF molecule show that for transitions involving P orbitals the model puts most of the intensity into perpendicular rather than parallel transitions.

The ground electronic state of an alkali halide has an ionic structure, M^+X^-, and since the molecule photodissociates into atoms, the pumping transition transition transfers an electron from X^- to M^+. We ignore all other electrons, and assume the valence electron which "jumps" goes from an $(np)_X$ atomic orbital centered on the halogen to an excited $(n'p)_M$ orbital centered on the alkali atom.

In general terms, the model assumes the wavefunctions for the initial and final states are separable as

$$\psi_i = \phi_i \text{ (jumping electron) } \phi \text{ (others)}$$

$$\psi_f = \phi_f \text{ (jumping electron) } \phi \text{ (others)},$$

where ϕ_i and ϕ_f are orthogonal one-electron orbitals. For this model the electronic transition dipole moment[22] is therefore given by

$$\underset{\sim}{\mu}_{if} = e \int \phi_i^* \underset{\sim}{r} \phi_f \, d\tau, \tag{22}$$

where $\underset{\sim}{r}$ is the coordinate vector of the valence electron.

The one-electron orbital functions are formed from a linear combination of atomic orbitals centered on the nuclei A(the alkali metal) and B(the halogen),

$$\phi_i = (\phi_A + \beta\phi_B)/N_i \tag{23}$$

$$\phi_f = (\alpha\phi_A - \phi_B)/N_f$$

The parameter β measures the probability of finding the valence electron on the B atom, the halogen atom, in the ground state; for a "covalent bond" between identical atoms $\beta = 1$ whereas for an "ionic bond" $\beta >> 1$. Similarly, the parameter α measures the probability that the valence electron is on the A atom, the alkali atom, in the excited state; again $\alpha = 1$ for a covalent bond and $\alpha >> 1$ for an ionic bond. The constants α and β are related by the requirement that ϕ_i and ϕ_f be orthogonal, and N_i and N_f are normalization factors. Thus we have

$$\beta = (S_{AB} - \alpha)/(\alpha S_{AB} - 1) \tag{24}$$

$$N_i = (1 + \beta^2 + 2\beta S_{AB})^{1/2} \tag{25}$$

$$N_f = (1 + \alpha^2 - 2\alpha S_{AB})^{1/2} \tag{26}$$

where

$$S_{AB} = \int \phi_A^* \phi_B d\tau \tag{27}$$

measures the overlap of the atomic orbitals.

According to (22) and (23) the transition dipole moment is given by

$$\underset{\sim}{\mu}_{if} = \frac{e}{N_i N_f} \left[\alpha \langle \underset{\sim}{r} \rangle_A - \beta \langle \underset{\sim}{r} \rangle_B + (\alpha\beta - 1) \langle \phi_A | \underset{\sim}{r} | \phi_B \rangle\right], \tag{28}$$

where

$$\langle \underset{\sim}{r} \rangle_A = \int \phi_A^* \, \underset{\sim}{r} \, \phi_A \, d\tau \tag{29a}$$

$$\langle \underset{\sim}{r} \rangle_B = \int \phi_B^* \, \underset{\sim}{r} \, \phi_B \, d\tau \tag{29b}$$

and

$$\langle \phi_A | \underset{\sim}{r} | \phi_B \rangle = \int \phi_A^* \, \underset{\sim}{r} \, \phi_B \, d\tau. \tag{30}$$

Although the magnitude of the individual terms in (28) depends upon the choice of the origin of the coordinate system, the net result does not.[22] Since we take the origin on the B atom (the halogen) and pass the z-axis through the A atom (the alkali atom),

$$\langle \underset{\sim}{r} \rangle_B = 0, \tag{31}$$

and

$$\langle x\rangle_A = \langle y\rangle_B = 0, \tag{32}$$

$$\langle z\rangle_A = r_o, \text{ the bond distance.} \tag{33}$$

Thus the first two terms in (28) contribute only to parallel transitions.

If the molecule is homopolar and both the initial and final states for the transition are "purely covalent," we have $\alpha = \beta = 1$, and the third term vanishes. Hence in this limit the model predicts that perpendicular transitions have negligible intensity; for parallel transitions it gives

$$\mu_z(\alpha=\beta=1) = \frac{er_o}{2(1-S^2)} . \tag{34}$$

This agrees with a formula derived by Mulliken and Herzberg[22] for the $\sigma_g 1s \rightarrow \sigma_u 1s$ transition in H_2^+. If r_o is not too small, the square of the overlap integral is small compared to unity, and the transition moment is roughly equal to the dipole moment of an electron oscillating with an amplitude $r_o/2$.

If both the initial and final states for the transition are "ionic," we have $\alpha >> 1$, $\beta >> 1$. In this limit, $\phi_i \simeq \phi_B$ and $\phi_f \simeq \phi_A$ and (28) gives

$$\mu_z(\alpha>>1,\beta>>1) \simeq \frac{er_o}{\beta} + e\langle\phi_A|z|\phi_B\rangle \tag{35}$$

$$\mu_\perp(\alpha>>1,\beta>>1) \simeq e\langle\phi_A|x \text{ or } y|\phi_B\rangle \tag{36}$$

Since the factor

$$\frac{1}{\beta} \simeq \frac{1-\alpha S}{\alpha}$$

in the first term of (35) is quite small, the relative importance of parallel and perpendicular transitions depends primarily on the ratio of the two-center dipole integrals

$$\langle \phi_A | z | \phi_B \rangle \text{ and } \langle \phi_A | x | \phi_B \rangle .$$

For the alkali halide molecules of interest here, the initial state is ionic, $\beta \gg 1$, whereas the final state is essentially covalent. However, $\alpha \neq 1$ since the bond is heteropolar, and from (24) we expect α to be of the order of $1/S$, which is also substantially greater than unity. Thus we shall consider the limiting case given in (35) and (36). If ϕ_A is an np orbital and ϕ_B an n'p orbital, there are only four types of nonvanishing two-center dipole integrals:

$$\langle np_z | z | n'p_z \rangle \tag{37a}$$

$$\langle np_x | z | n'p_x \rangle = \langle np_y | z | n'p_y \rangle \tag{37b}$$

$$\langle np_x | x | n'p_z \rangle = \langle np_y | y | n'p_z \rangle \tag{37c}$$

$$\langle np_z | x | n'p_x \rangle = \langle np_z | y | n'p_y \rangle \tag{37d}$$

The integrals of types (a) and (b) correspond to parallel transitions, and those of types (c) and (d) to perpendicular transitions. The integrals of types (b) and (c) have the same value, since

$$z | n'p_x \rangle = x | n'p_z \rangle$$

for any n'. (The factors $\langle np_x | z$ and $\langle np_z | x$ in the integrands of (b) and (c) are not the same, however, since the origin of the $\underset{\sim}{r}$ vector is on atom B). Thus we need to compare the magnitudes of only three integrals,

$$I_{zz} = \langle np_z | z | n'p_z \rangle \tag{37a}$$

$$I_{xz} = \langle np_x | x | n'p_z \rangle \tag{37b,c}$$

$$I_{zx} = \langle np_z | x | n'p_x \rangle \tag{37d}$$

Numerical calculations have been carried out for the LiF molecule, since the integrations are easily carried out for the $n = n' = 2$ case. Slater's rules[23] for approximate atomic orbitals give

$$\langle 2p_z | = Nze^{-Cr/z} \text{ and } \langle 2p_x | = Nxe^{-Cr/2} \tag{38}$$

The effective nuclear charge is

$$C = 1.3 \text{ for Li, } C = 5.2 \text{ for F,}$$

and the normalization constant is $N = (C^5/32\pi)^{1/2}$. All distances are measured in units of Bohr radii. The required integrals,

$$I_{zz} = \langle 2p_z(\text{Li}) | z | 2p_z(\text{F}) \rangle$$

$$I_{xz} = \langle 2p_x(\text{Li}) | x | 2p_z(\text{F}) \rangle$$

$$I_{zx} = \langle 2p_z(\text{Li}) | x | 2p_x(\text{F}) \rangle$$

may be simplified by noting that the product of x with a $2p_z$ orbital is a $3d_{xz}$ orbital with a different normalization factor and effective nuclear charge, and the product of z with a $2p_z$ orbital is a $3d_{z2}$ orbital plus a term independent of angle. Thus in the integrands of I_{xz} and I_{zz} we have

$$x | 2p_z(C) \rangle = N' | 3d_{xz}(C') \rangle \tag{39}$$

and

$$z|2p_z(C)\rangle = \tfrac{1}{3}N'|3d_{z^2}(C')\rangle + \tfrac{1}{3}Nr^2e^{-Cr/2} \tag{40}$$

where

$$N' = N_{2p}/N_{3d} = 81/8C \text{ and } C' = \tfrac{3}{2}C.$$

Since $\underset{\sim}{r}$ is measured from the F atom as the origin, C = 5.2 in these expressions. However, the x-coordinate of the electron is the same whether measured from the Li or the F atom as origin, and this enables us to evaluate the I_{zx} integral in the same way as I_{xz}, but with C = 1.3. The dipole integrals therefore reduce to

$$I_{zz} = \tfrac{1}{3}N_B'\langle 2p_z|3d_{z^2}\rangle + \tfrac{1}{3}N_AN_B\int r_A\cos\theta_A\ r_B^2e^{-\frac{1}{2}(C_Ar_A+C_Br_B)}d\tau \tag{41}$$

$$I_{xz} = N_B'\langle 2p_x|3d_{xz}\rangle \tag{42}$$

$$I_{zx} = N_A'\langle 3d_{xz}|2p_x\rangle\ . \tag{43}$$

Here A refers to the Li atom, B to the F atom. The terms involving N' are standard overlap integrals, and the remaining integral is readily evaluated from Coulson's tabulation of closed forms for certain two-center integrals,[24] since

$$\int r_a\ \cos\theta_A r_B^2e^{-\frac{1}{2}(C_Ar_A+C_Br_B)}d\tau = -2\ \frac{\partial}{\partial C_B}\ J_{14}(\tfrac{C_A}{2},\tfrac{C_B}{2},r_o) \tag{44}$$

where J_{14} is an integral given explicitly by Coulson,

$$J_{14}(A,B,R) = \int r_A r_B \cos\theta_A e^{-(Ar_A - Br_B)} d\tau$$

$$= \frac{8\pi}{R^2X^5} \left\{ \begin{array}{l} 4A[6(A^2+7B^2)(1+BR)-(A^2+11B^2)XR^2+BX^2R^3]e^{-BR} \\ -[24A(A^2+7B^2)(1+AR)+8A(A^2+5B^2)XR^2+(A^2+3B^2)X^2R^3]e^{-AR} \end{array} \right\}, \tag{45}$$

with $X = A^2 - B^2$. The numerical results are given in Table IV. Values of the overlap integrals are also included. The plus sign indicates that the term er_o/β (which is about $7.5/\beta$ Debye unites at the equilibrium internuclear distance,[25] where $r_o = 1.56$ Å) in Eq. (35) should be added to the listed values for the parallel transition moments.

Table IV. Results of charge transfer model for LiF transitions.

Transition Type	M Orbital		X Orbital	μ_{if} Debyes[a]	Overlap S_{MX}
Parallel	$2p_z$	←	$2p_z$	0.039+	0.069
Eq. (35)	$2p_x$	←	$2p_x$	0.973+	0.119
	$2p_y$	←	$2p_y$	0.973+	0.119
Perpendicular	$2p_x$	←	$2p_z$	0.973	zero
Eq. (36)	$2p_y$	←	$2p_z$	0.973	zero
	$2p_z$	←	$2p_x$	6.82	zero
	$2p_z$	←	$2p_y$	6.82	zero

[a]The integrals of Eqs. (41,42,43) are $eI_{zz} = 0.039$, $eI_{xz} = 0.973$, and $eI_{zx} = 6.82$. For comparison, $er_o = 7.48$ Debye units at the equilibrium internuclear distance, $r_o = 1.56$ Å.

The reason for the result $I_{zx} > I_{xz} >> I_{zz}$ becomes apparent in Figs. 6-8 which present contour maps of the factors L and R in the integrands of Eqs. (41-43):

	L(on left)	R(on right)	$\int LRd\tau$
Fig. 6	$\langle 2p_z(Li)\|x$	$\|2p_x(F)\rangle$	I_{zx}
Fig. 7	$\langle 2p_x(Li)\|$	$x\|2p_z(F)\rangle$	I_{xz}
Fig. 8	$\langle 2p_z(Li)\|$	$z\|2pz(F)\rangle$	I_{zz}

The contours are plotted for values of the coordinates such that

$$|f|^2/|f|^2_{max} \text{ or } |g|^2/|g|^2_{max} = 0.1,\ 0.3,\ 0.5,\ 0.7, \text{ and } 0.9$$

In each figure the Li atom is on the left and separated from the F atom by the equilibrium internuclear distance. Figs. 6 and 7 show that the L and R factors overlap constructively in I_{zx} and I_{xz}, whereas in Fig. 8 the R factor is completely surrounded by one lobe of the L factor and consequently there is extensive cancellation in the integrand of I_{zz}.

Although calculations have not been carried out for the $np(M) \longleftarrow n'p(X)$ transitions of other alkali halides, the present model is expected to give results similar to Table IV for all the alkali halides. The overlaps which determine the transition dipoles depend mainly on the relative scale and the separation of the M and X orbitals. Since the effective nuclear charge parameters C_M and C_X remain about the same for all the alkali halides and since the increase in bond length with size of M or X is offset by the expansion in scale which accompanies an increase in n or n', we expect the pattern found in Table IV to be typical.

The one-electron transfer model is severely oversimplified, of course. Perhaps its most realistic aspect is that it makes the transition dipole moment extremely sensitive to the type of bond and the transition considered, as illustrated in Eqs. (34-36) and Table IV. In particular, the weight given to perpendicular transitions in Table IV should be emphasized. This contradicts some "intuitive" versions of the charge transfer model, including one cited in our previous paper.[1]

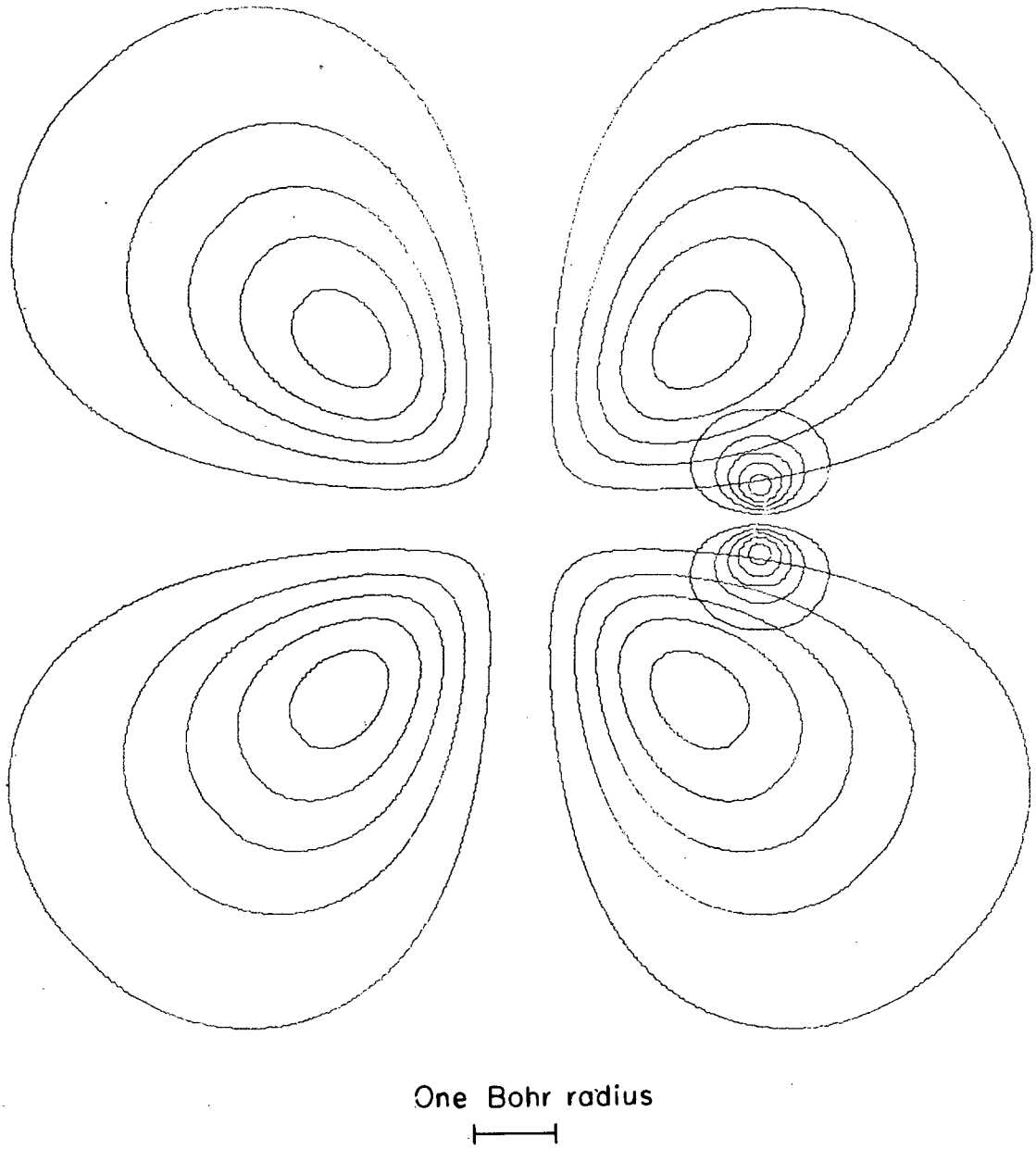

MUB-1839

Fig. 6. Contour map of factors $\langle 2p_z(\mathrm{Li})|x$ and $|2p_x(\mathrm{F})\rangle$ in the integrand of I_{zx} integral.

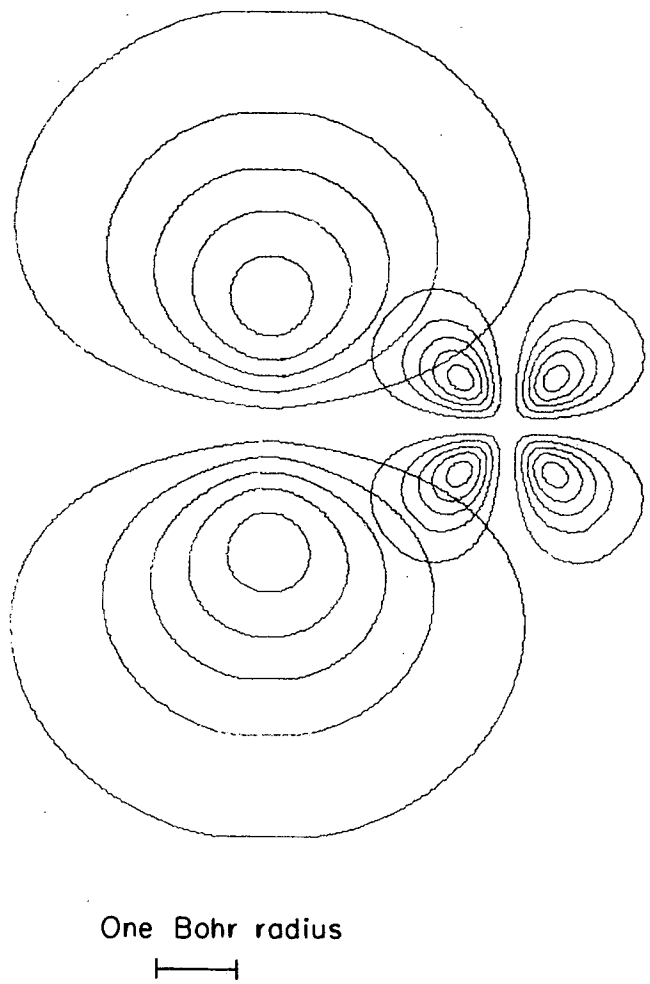

MUB-1836

Fig. 7. Contour map of factors $\langle 2p_x(Li)|$ and $x|2p_z(F)\rangle$ in the integrand of I_{xz} integral.

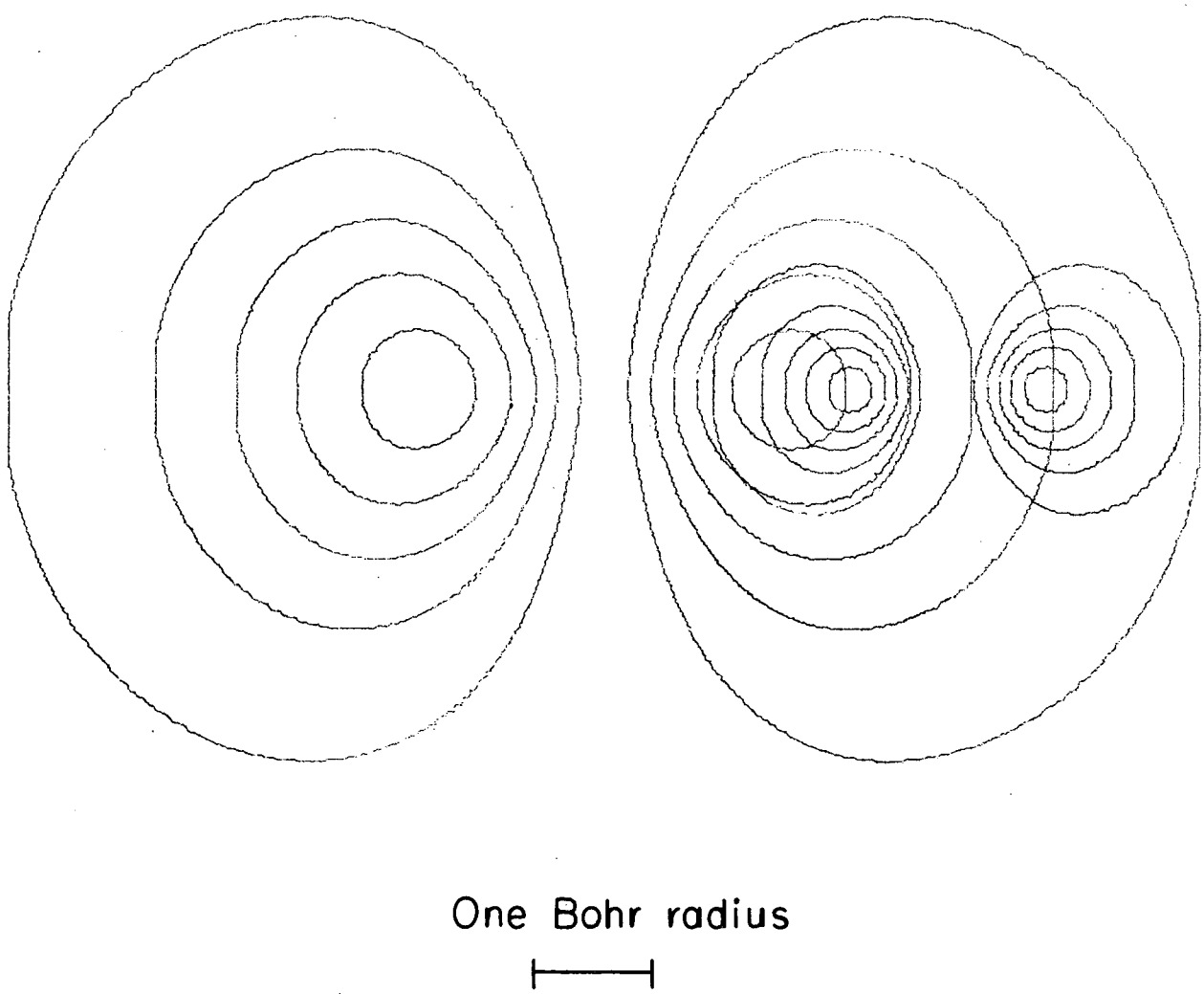

MUB-1837

Fig. 8. Contour map of factors $\langle 2p_z(\mathrm{Li})|$ and $z|2p_z(\mathrm{F})\rangle$ in the integrand of I_{zz} integral.

DETAILS OF COMPUTER PROGRAMS

The IBM 7090 FORTRAN programs which were prepared for the calculation of statistical weights and trajectories are given in Appendices I and II. The overlap integrals used in calculating the transition moments were evaluated by means of a SHARE subroutine, D1 MI D1AT. The XY plotting program used to prepare Figs. 6-8 is a modified version of another standard subroutine, J6 BC XYP2. Both of these subroutine programs are available at the University of California Computing Center, Berkeley.

APPENDIX I

```
C     HISTOGRAM CALCULATION FOR STATISTICAL WEIGHTS
      DIMENSION FR(30),BOX(60,4),FOX(60)
      DO 1 I = 1,60
      FOX(I) = 0.0
      DO 1 J = 1,4
1     BOX(I,J) = 0.0
      R = 2.7115E-8
      B = .1177
      RSTART = 2.4615E-8
      C = 3.0E+10
      VIN = 42105.0
      H = 6.62E-27
      A = 6.023E+23
      PI = 3.1415962
      HBAR = H/(PI*2.0)
      OMEGA = 2.86E+2
      U = 19.4692
      ALPHA = 4.0*PI**2*U*OMEGA*C/(H*A)
      QALPH = SQRTF(ALPHA/PI)
      C0 = QALPH
      C1 = QALPH/2.0
      C2 = QALPH/8.0
      C3 = QALPH/48.0
      T = 854.0
      DO 50 J = 1,121,5
      JI = 1+(J-1)/5
   50 FR(JI) = 1.4387*B/T*EXPF((-2.8589E-3)*B*FLOATF(J*(J+1))/(T*1.9872E
     1 -3))
      W0 = 100.0
      W1 = 61.9
      W2 = 38.4
      W3 = 23.9
      SULK = SQRTF(ALPHA)
      DO 51 J = 1,121,5
      JI = 1 + (J-1)/5
      DO 51 K = 0,100
      XC  = RSTART + FLOATF(K)*5.0E-11
      XCM = XC - R
      X = XCM*SULK
      XUP = (XC -RSTART)*1.0E+8
      H1Q = (2.0*X)**2
      H2Q = (4.0*X**2-2.0)**2
      H3Q = (8.0*X**3-12.0*X)**2
      XP = EXPF(-(ALPHA*XCM**2))
      VR = 3.9549354E+6*XUP**6 - 6.7053816E+6*XUP**5 + 4.250458E+6*XUP**
     1 4 - 1.2435592E+6*XUP**3 + 1.9445371E+5*XUP**2 - 3.7670057E+4*XUP
     2 + 4.9953698E+4
      E = VR-VIN+.5*FLOATF(J**2)*HBAR*A*(HBAR/(U*XC**2*1.6E-12)*8067.0)
      VNA = U/22.991*SQRTF(2.0*E*A*1.6E-12/(8067.0*U))
      DER = 6.0*3.9549354E+6*XUP**5-5.0*6.7053816E+6*XUP**4+4.0*4.250458
     1E+6*XUP**3-3.0*1.2435592E+6*XUP**2+2.0*1.9445371E+5*XUP-3.7670057
     2E+4
      DERIV = DER-(FLOATF(J*J)*(H*A)*H/(U*XC**3*1.6E-12)*8067.0)
      ZJACOB = ABSF(2.0*E/(VNA*DERIV))
      STAT0 = C0*XP*W0*FR(JI)*ZJACOB
```

```
      STAT1 = C1*XP*W1*FR(JI)*H1Q*ZJACOB
      STAT2 = C2*XP*W2*FR(JI)*H2Q*ZJACOB
      STAT3 = C3*XP*W3*FR(JI)*H3Q*ZJACOB
      I = 1
      TEST = 5.0E+3
4     IF(VNA-TEST)2,2,3
2     BOX(I,1) = BOX(I,1) + STAT0
      BOX(I,2) = BOX(I,2) + STAT1
      BOX(I,3) = BOX(I,3) + STAT2
      BOX(I,4) = BOX(I,4) + STAT3
      GO TO 44
3     I = I + 1
      TEST = TEST + 5.0E+3
      GO TO 4
44    ANGST = 1.0E+8/VR
      FACE = VNA/(2.0*ANGST)
      STAT0 = STAT0*FACE
      I = 1
      TEST = 1950.0
444   IF(ANGST-TEST)22,22,23
22    FOX(I) = FOX(I) + STAT0
51    CONTINUE
      GO TO 4444
23    I = I + 1
      TEST = TEST + 10.0
      GO TO 444
4444  DIV = 0.0
      DDIV = 0.0
      DO 45 I = 1,60
      DIV = MAX1F(DIV,ABSF(BOX(I,1)))
45    DDIV = MAX1F(DDIV,ABSF(FOX(I)))
      DO 46 I = 1,60
      FOX(I) = FOX(I)/DDIV
      DO 46 J = 1,4
46    BOX(I,J) = BOX(I,J)/DIV
      WRITE OUTPUT TAPE 3,52
52    FORMAT(12H1 HISTOGRAMS///1X,1HJ,3H  I,8X,9HSTAT. WT.//)
      DO 47 J = 1,4
      DO 47 I = 1,60
47    WRITE OUTPUT TAPE 3,55,J,I,BOX(I,J)
55    FORMAT(I2,I3,5X,F8.4)
      WRITE OUTPUT TAPE 3,1010
1010  FORMAT(8H1 LAMBDA,7X,9HSTAT. WT.//)
      DO 48 I = 1,60
      X = 1950.0+FLOATF(I-1)*10.0
48    WRITE OUTPUT TAPE 3,56,X,FOX(I)
56    FORMAT(F8.2,5X,F8.4)
      CALL EXIT
      END
```

APPENDIX II

```
      TRAJECTORY CALCULATIONS

      DIMENSION FR(20),C(10),T(10),W(10),S(100),SI(100)
      WRITE OUTPUT TAPE 3, 24
24    FORMAT(23H1 CALCULATIONS FOR NAI   )
      R = 2.7115E-8
      B = .1177
      RSTART = 2.4615E-8
      H = 6.627E-27
      A = 6.023E+23
      VIN = 42105.0
      PI = 3.14159629
      HBAR = H/(PI*2.0)
      U = 19.4692
      T = 854.0
      DO 50 J=1,91,10
      JI = 1+(J-1)/10
50    FR(JI) = 1.4387*B/T*EXPF(-2.8589E-3*B*FLOATF(J*(J+1))/(T*1.9872E-3
     1))
      CONS = 1.0E-8
      CONV = 360.0/(2.0*PI)
      DELTA = 1.0E-10/3.0
      R1 = R + .55*CONS
      V0 = 0.0
      V1H= -.10
      V1L=  .15
      V2H= -.15
      V2L=  .20
      V3H= -.19
      V3L=  .25
      V4H= -.22
      V4L=  .28
      C(1) = 4.9953698E+4
      C(2) =-3.7670057E+4
      C(3) = 1.9445371E+5
      C(4) =-1.2435592E+6
      C(5) = 4.2504580E+6
      C(6) =-6.7053816E+6
      C(7) = 3.9549354E+6
      T(1) = V4H * CONS
      T(2) = V3H * CONS
      T(3) = V2H * CONS
      T(4) = V1H * CONS
      T(5) = V0  * CONS
      T(6) = V1L * CONS
      T(7) = V2L * CONS
      T(8) = V3L * CONS
      T(9) =V4L*CONS
      W(1) = 14.9
      W(2) = 23.9
      W(3) = 38.4
      W(4) = 61.9
      W(5) =100.0
      W(6) = 61.9
      W(7) = 38.4
      W(8) = 23.9
```

```
      W(9) = 14.9
      RQU = SQRTF(A/(2.0*U))
      DO 60 I=1,9
      DO 60 L=1,91,10
      JI = 1+(L-1)/10
      STAT = FR(JI)*W(I)
      X = (R-RSTART+T(I))/CONS
      IF(X-.52) 800,900,900
900   VR = VIN + 100.0
      GO TO 700
800   VR=0.0
      DO 70 J=2,7
70    VR = VR + C(J)*X**(J-1)
      VR = VR + C(1)
700   E = VR-VIN+.5*FLOATF(L**2)*HBAR*(A*HBAR)/(U*(R+T(I))**2*1.6E-12)*
     1 8066.03
      ABCON1 = FLOATF(L)*HBAR*RQU
      ZEE = FLOATF(L)*(HBAR*RQU)/(R1*SQRTF(E*1.6E-12/8066.03))
      ASYM = PI/2.0 - ATANF(SQRTF(1.0-ZEE**2)/ZEE)
      K=0
80    X=X+.01
      XK=X*CONS
      IF(.55-X) 90,90,200
200   IF(X-.52) 100,901,901
901   VR = 0.0
      GO TO 701
100   VR=0.0
      DO 110 J=2,7
110   VR = VR + C(J)*X**(J-1)
      VR = VR + C(1)-VIN
701   K=K+1
      S(K) = ABCON1/(SQRTF((E-VR)*1.6E-12/8066.03-FLOATF(L**2)*(HBAR*A)*
     1 HBAR/(U*(R+T(I)+XK)**2)*.5)*(R+T(I)+XK)**2)
      ST(K) = S(K) * (R+T(I)+XK)**2/(FLOATF(L)*HBAR)*U/A
      GO TO 80
90    ABCON2 = SQRTF(U/(2.0*A*E*1.6E-12/8066.03))
      K=K-1
      SUM=0.0
      STUM=0.0
      DO 120 J=2,K,2
      SUM = SUM +S(J-1) + 4.0*S(J) + S(J+1)
120   STUM = STUM + ST(J-1)+ 4.0*ST(J) + ST(J+1)
      ANGLE = DELTA * SUM
      TIME = DELTA * STUM
      CHI = (ANGLE + ASYM)*CONV
      WRITE OUTPUT TAPE 3,21,I,L,CHI,STAT
21    FORMAT(65H0 VIBRATION  ROTATION                CHI          STATISTICAL
     1 WEIGHT  /110,I10,1P2E20.8)
      SCHRD = SQRTF(R1**2-FLOATF(L**2)*HBAR*(A*HBAR)/(2.0*U*E*1.6E-12)*
     1 8066.03)
      WRITE OUTPUT TAPE 3,22
22    FORMAT(61H0                ANGLE              DISTANCE                T
     1IME   )
      WRITE OUTPUT TAPE 3,23,ANGLE,R1,TIME
23    FORMAT(1P3E20.8)
      STP=0.0
      DIST = 4.0*CONS
130   DIST = DIST + STP
      ZE = ZEE * R1 / DIST
      ANG = CHI - (PI/2.0-ATANF(SQRTF(1.0-ZE**2)/ZE))*CONV
      TIM = TIME + ABCON2*(SQRTF(DIST**2-FLOATF(L**2)*(HBAR*A)*HBAR/(2.0
```

```
     1 *U*E*1.6E-12)*8066.03) - SCHRD)
      WRITE OUTPUT TAPE 3,23,ANG,DIST,TIM
      STP = 1.0*CONS
      IF(DIST - 1.0E-7) 130,600,600
600   STP = 20.0*CONS
      IF(DIST-1.0E-6) 130,60,60
60    CONTINUE
      CALL EXIT
      END
```

References

1. R. N. Zare and D. R. Herschbach, Proc. I.E.E.E. 51, 173 (1963); also UCRL-10411 (August, 1962).
2. J. R. Singer and I. Gorog, Bull. Am. Phys. Soc. 7, 14 (1962).
3. S. G. Rautian and I. I. Sobelman, J. Exptl. Theoret. Phys. 14, 1433 (1962).
4. H. G. Hanson, J. Chem. Phys. 27, 491 (1957).
5. E. U. Condon, Am. J. Phys. 15, 365 (1947).
6. J. W. Cooley, Math. of Computation 15, 365 (1947).
7. J. G. Winans and E. C. G. Stueckelberg, Proc. Nat. Acad. Amer. 14, 867 (1928).
8. A. S. Coolidge, H. M. James, and R. D. Present, J. Chem. Phys. 4, 193 (1936).
9. See, for example, L. Pauling and E. B. Wilson, Introduction to Quantum Mechanics (McGraw-Hill, New York, 1935), pp. 77-81.
10. H. G. Hanson, J. Chem. Phys. 23, 1391 (1955).
11. L. Brewer and E. Brackett, Chem. Rev. 61, 425 (1961).
12. A. G. Gaydon, Dissociation Energies and Spectra of Diatomic Molecules (Chapman and Hall, London, 1953).
13. G. Herzberg, Spectra of Diatomic Molecules (D. Van Nostrand Co., Inc., New York, 1950).
14. C. E. Moore, Atomic Energy Levels, Vols. I, II, III, Circular 467, National Bureau of Standards (Washington, D.C., 1949, 1952, 1958).
15. P. Pringsheim, Fluorescence and Phosphorescence (Interscience Publishers, Inc., New York, 1949), pp. 275-279.
16. E. Wigner and E. E. Witmer, Z. Physik 51, 859 (1928).
17. R. S. Mulliken, Phys. Rev. 36, 1440 (1930).
18. A. Terenin, Physica 10, 209 (1930).

References (Continued)

19. D. R. Bates, R. T. S. Darling, S. C. Hawe, and A. L. Stewart, Proc. Phys. Soc. A66, 1124 (1953).

20. R. S. Mulliken, Phys. Rev. 50, 1017, 1028 (1936); 51, 310 (1937).

21. A. C. G. Mitchell, Z. Physik 49, 228 (1928).

22. Reference 13, pages 199-201, 381-386.

23. J. C. Slater, Phys. Rev. 36, 57 (1930).

24. C. A. Coulson, Proc. Camb. Phil. Soc. 38, 210 (1942).

25. L. Wharton, W. Klemperer, L. P. Gold, R. Strauch, J. J. Gallagher, and V. E. Derr, J. Chem. Phys. 38, 1203 (1963).

This report was prepared as an account of Government sponsored work. Neither the United States, nor the Commission, nor any person acting on behalf of the Commission:

A. Makes any warranty or representation, expressed or implied, with respect to the accuracy, completeness, or usefulness of the information contained in this report, or that the use of any information, apparatus, method, or process disclosed in this report may not infringe privately owned rights; or

B. Assumes any liabilities with respect to the use of, or for damages resulting from the use of any information, apparatus, method, or process disclosed in this report.

As used in the above, "person acting on behalf of the Commission" includes any employee or contractor of the Commission, or employee of such contractor, to the extent that such employee or contractor of the Commission, or employee of such contractor prepares, disseminates, or provides access to, any information pursuant to his employment or contract with the Commission, or his employment with such contractor.